THE JOURNAL OF BIOLOGICAL CHEMISTRY
Vol. 277, No. 46, Issue of November 15, pp. 44268–44277, 2002
Printed in U.S.A.

Structural and Functional Consequences of Mutating Cysteine Residues in the Amino Terminus of Human Multidrug Resistance-associated Protein 1*

Received for publication, July 12, 2002, and in revised form, August 22, 2002
Published, JBC Papers in Press, September 13, 2002, DOI 10.1074/jbc.M207003200

Youyun Yang, Qun Chen, and Jian-Ting Zhang‡

From the Department of Pharmacology and Toxicology, Walther Oncology Center/Walther Cancer Institute and the Indiana University Cancer Center, Indiana University School of Medicine, Indianapolis, Indiana 46202

Multidrug resistance-associated protein 1 (MRP1) is a member of the ATP-binding cassette membrane transport superfamily and is responsible for multidrug resistance in cancer cells. Currently, there are nine known human MRPs. Distinct from many other members of the ATP-binding cassette superfamily, human MRP1 and four other MRPs have an additional membrane-spanning domain (MSD) with a putative extracellular amino terminus. The functional significance of this additional MSD (MSD1) is currently unknown. To understand the role of MSD1 in human MRP1 structure and function, we studied the amino-terminal 33 amino acids. We found that the amino terminus of human MRP1 has two cysteine residues (Cys^7 and Cys^{32}) that are conserved among the five human MRPs that have MSD1. Mutation analyses of the two cysteines in human MRP1 revealed that the Cys^7 residue is critical for the MRP1-mediated drug resistance and leukotriene C_4 transport activity. On the other hand, mutation of Cys^{32} reduced only moderately the MRP1 function. The effect of Cys^7 mutation on MRP1 activity appears to be due to the 5–7-fold decrease in the maximal transport rate V_{max}. We also found that mutation of Cys^7 changed the amino-terminal conformation of MRP1. This conformational change is likely responsible for the decrease in V_{max} of LTC_4 transport mediated by the mutant MRP1. Based on these studies, we conclude that the amino terminus of human MRP1 is important and that the Cys^7 residue plays a critical role in maintaining the proper structure and function of human MRP1.

Human multidrug resistance-associated protein 1 (MRP1),[1] also named ABCC1 (refer to www.gene.ucl.ac.uk/nomenclature/genefamily/abc.html for complete nomenclature) is a multiple-drug membrane efflux pump that causes multidrug resistance in human cancer chemotherapy (1). It belongs to the ATP-binding cassette membrane transport superfamily, which includes various transporters with a wide variety of substrates (2–5). Currently, there are nine known human MRP transporters (1, 4, 6–11), and human MRP1 has been shown to have clinical relevance to the multidrug resistance of human cancers (12).

Of the nine human MRPs, MRP1, MRP2, MRP3, MRP6, and MRP7 have different membrane organization from the other human MRPs and from most of other known human ATP-binding cassette transporters such as P-glycoprotein (ABCB1) and CFTR (ABCC7). They have an extra membrane-spanning domain (MSD) in addition to the traditional core structure consisting of two nucleotide-binding domains and two MSDs (see Fig. 1*A*). This additional MSD (MSD1) shows a low overall amino acid identity among the members that have this domain, but it may be structurally conserved (13). It consists of five putative transmembrane segments with an amino terminus that has been suggested to be extracellular by determining glycosylation status (14, 15), by epitope insertion (16), and by cell-free expression in microsomal membranes (17). However, the extracellular location of the amino terminus of MSD1 has recently been questioned using a monoclonal antibody generated against the amino terminus of human MRP1 (18) (see Fig. 1*B*).

It is currently unknown whether MSD1 is functionally important. Gao *et al.* (19) showed that partial deletion of MSD1 (as little as the amino-terminal 66 amino acids including the first transmembrane segment) reduced 90% of the LTC_4 transport activity of human MRP1. On the other hand, Bakos *et al.* (20) found that human MRP1 lacking the entire MSD1 is still functional in transporting substrates such as LTC_4. However, both groups found that the loop (L_0) linking MSD1 and MSD2 is functionally important (19–21). Together with these results, the novel finding that the amino terminus of human MRP1 may be intracellular (18) makes it interesting to investigate the importance of the amino terminus in both the structural and functional integrity of human MRP1.

To this end, we investigated the importance of the amino-terminal 33 amino acids in the structure and function relationship of human MRP1. Examination of the amino termini of human MRP1, 2, 3, 6, and 7 revealed that there are two cysteine residues (Cys^7 and Cys^{32} in human MRP1) at the amino terminus that are conserved among the five human MRPs and mouse mrp1 (see Fig. 1*A*). In this study, we mutated these two cysteines of human MRP1 to alanine individually or in combination and investigated the effect of these mutations on MRP1 function and conformation. We found that mutation of Cys^7 reduced ~80% of MRP1-mediated drug resistance and LTC_4 transport, whereas mutation of Cys^{32} reduced only ~20–40% of MRP1 function. The effect of Cys^7 mutation on drug

* This work was supported in part by National Institutes of Health Grants CA64539 and GM59475 and by Department of Defense Grant DAMD170010297. The costs of publication of this article were defrayed in part by the payment of page charges. This article must therefore be hereby marked "*advertisement*" in accordance with 18 U.S.C. Section 1734 solely to indicate this fact.

‡ Recipient of a Career Investigator Award from the American Lung Association. To whom correspondence should be addressed: Dept. of Pharmacology and Toxicology, IUCC, Indiana University School of Medicine, 1044 W. Walnut St., R4-166, Indianapolis, IN 46202. Tel.: 317-278-4503; Fax: 317-274-8046; E-mail: jianzhan@iupui.edu.

[1] The abbreviations used are: MRP1, multidrug resistance-associated protein 1; MSD, membrane-spanning domain; LTC_4, leukotriene C_4; FITC, fluorescein isothiocyanate; PBS, phosphate-buffered saline; PMSF, phenylmethylsulfonyl fluoride; DTT, dithiothreitol; FACS, fluorescence-activated cell sorter.

transport appears to be due to a 5–7-fold decrease in the maximal transport rate V_{max}. This change is likely due to the conformational alteration of the amino terminus caused by the mutation of Cys^7. Based on these results, we conclude that the amino terminus of human MRP1 is important and that the Cys^7 residue plays a critical role in maintaining the proper structure and function of human MRP1.

EXPERIMENTAL PROCEDURES

Materials—[^{3}H]LTC_4 was purchased from PerkinElmer Life Sciences. LTC_4, L-1-tosylamido-2-phenyethyl chloromethyl ketone-treated trypsin, peroxidase- and FITC-conjugated goat anti-mouse IgG, peroxidase-conjugated rabbit anti-rat IgG, doxorubicin, colchicine, vincristine, and VP16 (etoposide) were purchased from Sigma. LipofectAMINE and G418 were purchased from Invitrogen. Cell culture media, fetal bovine serum, penicillin, and streptomycin were from BioWhittaker. ECL reagent and polyvinylidene difluoride membranes were purchased from Amersham Biosciences and Bio-Rad, respectively. Monoclonal antibodies QCRL-1 and MRPr1 were obtained from Centocor and Kamiya Biomedical Company, respectively. All other chemicals were from Fisher or Sigma.

Engineering Human MRP1 Constructs—Mutations of Cys^7 and Cys^{32} to Ala were generated using the Transformer™ site-directed mutagenesis kit (Clontech, Palo Alto, CA). The cDNA template was prepared by cloning the *Bam*HI fragment encoding the first 281 amino acids of MRP1 from pRc/RSV-MRP (a gift from Dr. Piet Borst, Netherlands Cancer Institute, Amsterdam, The Netherlands) into the *Bam*HI site of pGEM-4Z. Mutagenesis was then performed according to the manufacturer's instructions using the selection primer 5′-pGTGCTCATCATTGGGAAACGTTCTTCGGG and the mutagenic primers 5′-pCCGGGGCTTCGCCAGCGCCGATG ($Cys^7 \rightarrow Ala$) and 5′-pCCGACTTCACCAAGGCCTTTCAGAACACGG ($Cys^{32} \rightarrow Ala$). The underlined nucleotides represent mutations. The *Nhe*I-*Bam*HI fragments containing the wild type or desired mutations from pGEM-4Z together with a *Bam*HI-*Not*I fragment from pRc/RSV-MRP were ligated into pcDNA3.1(+) vector linearized with *Nhe*I and *Not*I to create pcDNA3.1(+)-$MRP1^{WT}$, pcDNA3.1(+)-$MRP1^{C7A}$, pcDNA3.1(+)-$MRP1^{C32A}$, and pcDNA3.1(+)-$MRP1^{C7A/C32A}$.

To generate wild type and mutant pCEP4-$MRP1^{281N}$ constructs, the plasmids pcDNA3.1(+)-$MRP1^{WT}$, -$MRP1^{C7A}$, -$MRP1^{C32A}$, and -$MRP1^{C7A/C32A}$ were digested with *Bam*HI and blunted with Klenow followed by digestion with *Nhe*I. The *Nhe*I-*Bam*HI fragment encoding the first 281 amino acids of MRP1 were ligated to linearized pCEP4 vector with a cohesive *Nhe*I end and a blunted *Not*I end. Translation of the inserted fragment terminates at a stop codon in the vector, resulting in the addition of 16 amino acids (RPLEAGKAGSRHDKIH) following the amino acid residue Asp^{281} of human MRP1, similar to what was described in Refs. 19 and 20.

The human $MRP1^{CORE}$ construct was engineered by amplifying a 464-bp fragment of MRP1 using a forward primer with a *Nhe*I site (underlined) 5′-CTAGCTAGCGCCGCCATGGATCCTGCCCAGCCG-3′ and a reverse primer 5′-CACAGACATGAGGTTGAC-3′. The PCR product was then digested with *Nhe*I and *Psh*AI to generate a 365-bp fragment from nucleotides 976 to 1327 of MRP1, which was subcloned into pcDNA3.1(+)-$MRP1^{WT}$ digested with *Nhe*I and *Psh*AI, resulting in pcDNA3.1(+)-$MRP1^{CORE}$. To generate pCEP4-$MRP1^{CORE}$, the cDNA encoding amino acid residues 281–1531 of MRP1 was released from the pcDNA3.1(+)-$MRP1^{CORE}$ by *Nhe*I and *Not*I digestion and inserted into the pCEP4 vector, which was digested with *Nhe*I and *Not*I. All of the constructs and mutations described above were confirmed by automated DNA sequencing.

Cell Culture and Transfection of HEK293 Cells—HEK293 cells were grown in Dulbecco's modified Eagle's medium supplemented with 10% fetal bovine serum in the presence of 100 units/ml penicillin and 100 μg/ml of streptomycin. For stable transfection, 5 μg of pcDNA3.1(+)-$MRP1^{WT}$, -$MRP1^{C7A}$, -$MRP1^{C32A}$, or -$MRP1^{C7A/C32A}$ were transfected into HEK293 cells using LipofectAMINE according to the manufacturer's instructions. Two days following transfection, 10% of the transfected cells were selected with 400 μg/ml of G418 for 2 weeks. The G418-resistant cells were cloned using cloning cylinders and propagated for testing expression of wild type and mutant human MRP1.

For transient transfection, pCEP4-$MRP1^{281N}$ and/or pCEP4-$MRP1^{CORE}$ were transfected into HEK293 cells using LipofectAMINE according to the manufacturer's instructions. On the following day, tunicamycin was added to a final concentration of 2.5 μg/ml, and the cells were treated for 2 additional days before the cells were harvested for membrane preparations. Tunicamycin was used to eliminate heterogeneous glycosylation for convenience of detecting $MRP1^{281N}$ as a single sharp band rather than as a smear because of glycosylation on Western blot.

Membrane Preparation—The membrane vesicles were prepared as described previously with modifications (22, 23). Briefly, the cells were washed with ice-cold PBS and resuspended in hypotonic lysis buffer (10 mM KCl, 1.5 mM $MgCl_2$, 10 mM Tris-HCl, pH 7.4, 1 mM PMSF) at 1×10^6 cells/ml followed by homogenization and centrifugation at 4,000 × *g* for 10 min. Crude membranes were obtained by centrifugation of the 4,000 × *g* supernatant at 100,000 × *g* for 1 h. The crude membrane pellet was then resuspended in STBS (250 mM sucrose, 10 mM Tris-HCl, pH 7.4, 150 mM NaCl, 1 mM PMSF), passed through a 26-gauge needle for 20 times, aliquoted, and stored at −80 °C. The plasma membrane fractions were prepared by layering the 4,000 × *g* supernatant on top of a 35% sucrose cushion containing 10 mM Tris-HCl, pH 7.4, 1 mM EDTA, 1 mM PMSF followed by centrifugation at 100,000 × *g* for 1 h. The membranes at the interface between the supernatant and the sucrose cushion were collected and pelleted by centrifugation. The membrane pellet was washed with STBS, and then the vesicles were prepared as described above.

[^{3}H]LTC_4 Transport and Kinetic Parameter Measurement—The ATP-dependent transport of [^{3}H]LTC_4 into the inside-out plasma membrane vesicles was measured using a rapid filtration method as previously described (23). Briefly, 10-μg membrane vesicles were incubated at 23 °C in 120 μl of transport buffer (50 mM Tris-HCl, 250 mM sucrose, 0.02% sodium azide, pH 7.4) containing 4 mM ATP or AMP, 10 mM $MgCl_2$, 100 μg/ml of creatine kinase, 10 mM creatine phosphate, and 50 nM [^{3}H]LTC_4 (0.05 μCi). At each desired time point, a 20-μl aliquot was removed and mixed with 1 ml of ice-cold transport buffer, followed by filtration under vacuum through a glass fiber filter (Type GF/B, Whatman). The filters were immediately washed twice with 5 ml of ice-cold transport buffer and then dried before measurement of radioactivity by scintillation counting. The K_m and V_{max} values of ATP-dependent [^{3}H]LTC_4 transport by membrane vesicles were measured at various [^{3}H]LTC_4 concentrations (12.5–1600 nM) for 1 min at 23 °C in 25 μl of transport buffer followed by nonlinear regression analysis. The [^{3}H]LTC_4 uptake and the V_{max} value were corrected for the MRP1 expression level in each sample as previously described (20, 24–26).

Limited Trypsin Digestion—Limited trypsin digestion was performed as previously described (14, 15, 27–29). Briefly, 10-μg membranes were washed once with PBS. The pellets were resuspended in 30 μl of PBS with 1.5-μg of L-1-tosylamido-2-phenyethyl chloromethyl ketone-treated trypsin and incubated at 37 °C for 2 h. PMSF was then added to a final concentration of 10 mM to stop the reaction. The membrane proteins were collected by centrifugation at 12,000 × *g* for 15 min at 4 °C. The pellets were immediately solubilized in SDS-PAGE sample buffer (50 mM Tris-HCl, pH 6.8, 100 mM DTT, 2% SDS, 10% glycerol, and 0.1% bromphenol blue) and subjected to SDS-PAGE for Western blot analysis as described below.

Deglycosylation and Western Blot—Western blot was performed as previously described (22). Briefly, isolated membranes or membranes treated with Peptide N-glycosidase F (22) were solubilized in SDS-PAGE sample buffer at room temperature for 30 min and then subjected to SDS-PAGE and transferred to polyvinylidene difluoride membranes. For nonreducing SDS-PAGE, the samples were treated with SDS-PAGE sample buffer without DTT. The blots were then blocked with 10% milk and probed with monoclonal antibodies QCRL-1 (2.2 μg/ml) or MRPr1 (0.25 μg/ml) followed by horseradish peroxidase-conjugated goat anti-mouse IgG or horseradish peroxidase-conjugated rabbit anti-rat IgG (for MRPr1). The signal was detected using ECL.

Confocal Microscope Imaging—1×10^5 stably transfected HEK293 cells were seeded on a glass coverslip in a six-well tissue culture plate. After the culture reaches confluency, the cells were washed twice with ice-cold PBS and fixed with acetone/methanol (1:1) at room temperature for 10 min and incubated at 4 °C for 30 min with blocking solution (1% bovine serum albumin, 1% horse serum in PBS). The cells were then probed with primary antibody QCRL-1 (11 μg/ml) for 30 min at 4 °C followed by incubation with FITC-conjugated goat anti-mouse IgG $F(ab')_2$ fragment (Sigma) (1:100 dilution) at 4 °C for another 30 min. After being washed twice with blocking solution, the cell nucleus was counterstained with propidium iodide (25 μg/ml) for 10 min. The coverslips were then mounted on the slides before viewing with a confocal microscope.

Cytoxicity Assay—Cells were seeded in 96-well plates at 4×10^3 cells/well. After incubation at 37 °C overnight, the medium containing different concentrations of drugs was added to a final volume of 100 μl. The cells were then incubated for 3 days in the absence or presence of drugs followed by the addition of 3-(4,5-dimethylthiazol-2-yl)-2,5-diphe-

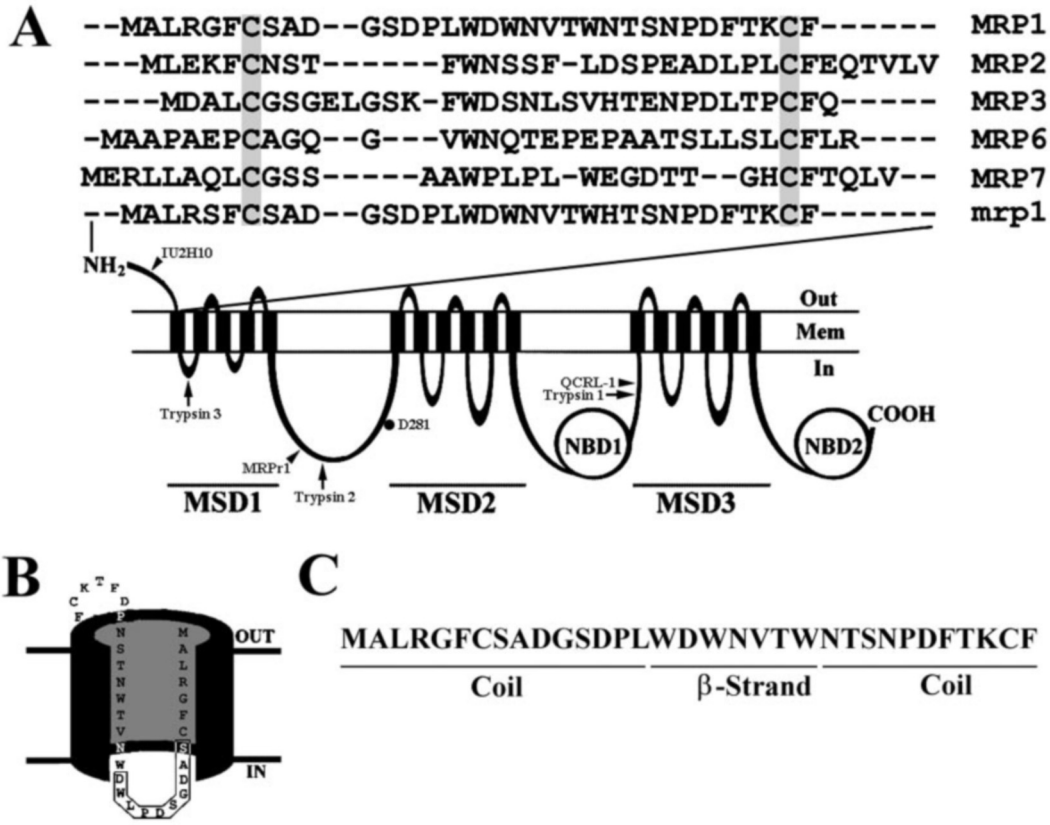

FIG. 1. **Sequence alignment of the amino termini of human MRP1, 2, 3, 6, and 7 and mouse mrp1 and the putative topology of human MRP1 with the predicted secondary structure of the amino terminus.** *A*, sequence alignment. The first 33 amino acids of human MRP1, 2, 3, 6, and 7 and mouse mrp1 are aligned using CLUSTALW at European Bioinformatic Institute (www.expasy.ch/tools/#sequence). The two conserved cysteine residues are *shaded*. The predicted topology of human MRP1 is shown schematically. The *filled boxes* are putative transmembrane segments, whereas the *open circles* are nucleotide-binding domains (*NBD*). The *arrows* indicate the putative trypsin digestion sites, and the *arrowheads* show the approximate epitope position for monoclonal antibodies used in this study (IU2H10, Ser^{8}–Asp^{17}; MRPr1, Gly^{238}–Glu^{247}; QCRL-1, Tyr^{918}–Arg^{924}). Asp^{281} is indicated by a *solid circle*. *B*, alternative folding of the amino terminus. The position of amino terminus in the putative channel is arbitrary. The *boxed sequence* is the IU2H10 epitope. *C*, predicted secondary structure of the amino terminus of human MRP1. It consists of mostly coiled structure with a stretch of β-strand as indicated.

nyltetrazolium bromide (5 mg/ml) to a final concentration of 0.5 mg/ml and incubation of the plates at 37 °C for 2 h. An equal volume (100 μl) of solubilization solution (10% SDS in 0.01 M HCl) was then added, and the plates were incubated at 37 °C overnight. The $A_{570\ nm}$ was measured using an automated plate reader. IC_{50} is defined as the concentration of drugs required to kill 50% of the cells in the control condition and was corrected for the MRP1 expression level as previously described (20, 24–26).

FACS Analysis—FACS analysis was performed at 4 °C as previously described (18). Briefly, the cells were aliquoted into a microtiter plate at the density of 0.5×10^6/well and were washed twice with wash buffer (1% bovine serum albumin in PBS). The cells were then blocked in blocking solution for 30 min followed by incubation with IU2H10 and QCRL-1 for 30 min in the presence of 0.2% saponin. The cells were then washed twice with wash buffer and incubated with FITC-conjugated goat anti-mouse IgG $F(ab')_2$ fragment in blocking solution for 30 min and then washed twice again with wash buffer. Finally, the cells were resuspended in 1% paraformaldehyde in PBS for 30 min and analyzed by FACS.

RESULTS

Expression of Wild Type and Mutant MRP1 in HEK293 Cells—Fig. 1*A* shows that the two cysteine residues (Cys^7 and Cys^{32}) in the amino terminus are conserved among human MRP1, 2, 3, 6, and 7 and mouse mrp1. To investigate whether these two cysteine residues are functionally important, we mutated them to alanine in human MRP1 and created $MRP1^{C7A}$, $MRP1^{C32A}$, and $MRP1^{C7A/C32A}$. These mutant and wild type human MRP1 cDNAs were cloned into the expression vector pcDNA3.1(+) and transfected into HEK293 cells. HEK293 cells were chosen because they have been used successfully in previous studies to express wild type and mutant human MRP1 for functional studies, and no detectable endogenous MRP1 were found in these cells (24–26, 30–33). The G418-resistant cells were cloned and tested for their expression of human MRP1 by Western blot. As shown in Fig. 2*A*, both wild type and mutant MRP1 were efficiently produced in MRP1-transfected HEK293 cells but at different levels as determined using MRP1-specific monoclonal antibody QCRL-1. However, the vector-transfected cells did not have detectable endogenous MRP1. Fig. 2*B* shows that both the wild type and mutant MRP1 were glycosylated to the same extent, suggesting that both wild type and mutant human MRP1 are properly routed and modified post-translationally. To further determine whether the mutant proteins were properly routed to the cell surface, we performed an indirect immunofluorescence staining of these cells with QCRL-1. As shown in Fig. 3, the cells expressing $MRP1^{WT}$, $MRP1^{C7A}$, $MRP1^{C32A}$, and $MRP1^{C7A/C32A}$ all showed plasma membrane staining. Based on the above observation, we conclude that mutations of cysteine residues in the amino terminus of human MRP1 do not affect the proper routing and trafficking of these proteins to the plasma membrane and their glycosylation in HEK293 cells.

Effect of Mutations of Cys^7 and Cys^{32} on Human MRP1-mediated [^{3}H]LTC_4 Transport—To determine whether the above mutations affect the function of human MRP1, we performed ATP-dependent [^{3}H]LTC_4 transport analysis using plasma membrane vesicles isolated from the cells expressing wild type and mutant human MRP1. As shown in Fig. 4, the

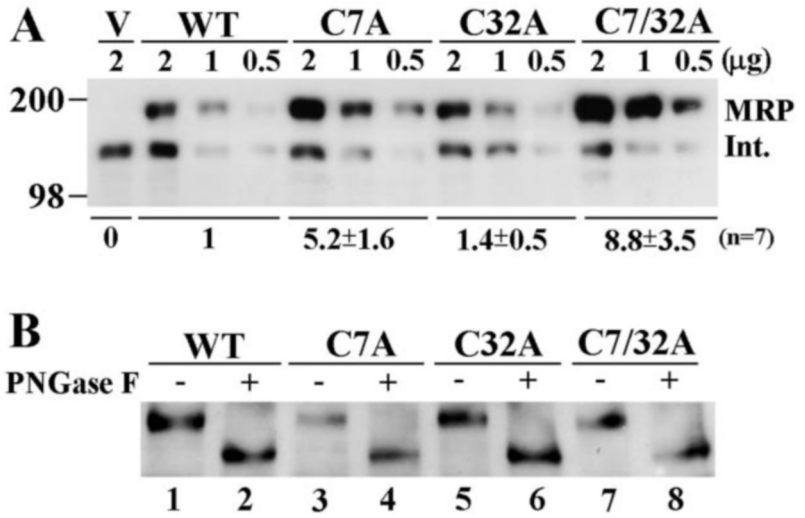

FIG. 2. **Expression and deglycosylation analysis of wild type and mutant human MRP1.** *A*, membrane proteins (2, 1, and 0.5 μg) from stable HEK293 cells transfected with vector (*V*), human MRP1^{WT}, MRP1^{C7A}, MRP1^{C32A}, and MRP1$^{C7A/C32A}$ were subjected to SDS-PAGE and Western blot analysis probed with monoclonal antibody QCRL-1. Integrin $\beta 1$ (*Int.*) was used as a loading control. The *numbers below* the blot show the relative amounts of human MRP1 expressed and were used for corrections in the functional studies. *B*, membrane proteins of human MRP1^{WT}, MRP1^{C7A}, MRP1^{C32A}, and MRP1$^{C7A/C32A}$ were treated with or without Peptide N-glycosidase F and then subjected to SDS-PAGE and Western blot analysis as in *A*. The protein molecular mass markers are indicated on the *left* in kDa.

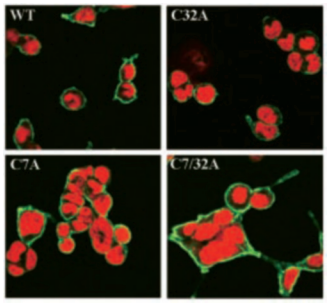

FIG. 3. **Indirect immunofluorescence staining of HEK293 cells expressing wild type and mutant human MRP1.** HEK293 cells expressing human MRP1^{WT}, MRP1^{C7A}, MRP1^{C32A}, and MRP1$^{C7A/C32A}$ grown on glass coverslips were stained with MRP1-specific monoclonal antibody QCRL-1 followed by incubation with a FITC-conjugated goat anti-mouse IgG F(ab′)$_2$ fragment. The nuclei were counterstained with propidium iodide.

[^{3}H]LTC$_4$ uptake profiles are very different between the wild type and mutant MRP1. The calculated initial transport rates for MRP1^{WT}, MRP1^{C7A}, MRP1^{C32A}, and MRP1$^{C7A/C32A}$ after correction for protein expression level were 35.9 ± 4.9, 6.0 ± 1.5, 26.5 ± 1.0, and 6.9 ± 1.5 pmol/mg/min, respectively. The corrected initial [^{3}H]LTC$_4$ transport rates of the mutant MRP1^{C7A}, MRP1^{C32A}, and MRP1$^{C7A/C32A}$ were about 17, 74, and 19% of that of MRP1^{WT}, respectively. This observation suggests that the Cys^7 residue is critical for the function of human MRP1 to transport LTC$_4$.

We next measured the [^{3}H]LTC$_4$ transport K_m and V_{max} of MRP1^{WT}, MRP1^{C7A}, MRP1^{C32A}, and MRP1$^{C7A/C32A}$. As shown in Table I, the K_m values of wild type and all of the mutant MRP1s were similar. However, the V_{max} of MRP1^{C7A} and MRP1$^{C7A/C32A}$ corrected for MRP1 expression level was 5–7-fold less than that of MRP1^{WT} and MRP1^{C32A}. This observation suggests that mutation of Cys^7 residue decreased the V_{max} but had no effect on K_m of the LTC$_4$ transport by human MRP1.

Effect of Cys^7 and Cys^{32} Mutations on Human MRP1-mediated Multidrug Resistance—The above studies showed that the Cys^7 residue is critical for human MRP1-mediated LTC$_4$ transport. We next examined the drug resistance profile of transfectants expressing MRP1^{WT}, MRP1^{C7A}, MRP1^{C32A}, and MRP1$^{C7A/C32A}$ to colchicine, doxorubicin, vincristine, and VP16 as described under "Experimental Procedures." The results are summarized as normalized relative resistance in Fig. 5. It appears that mutation of Cys^7 reduced the MRP1-mediated drug resistance to about 20% of the wild type MRP1 for all four drugs tested. On the other hand, mutation of Cys^{32} reduced the MRP1-mediated drug resistance to only 60–80% of the wild type MRP1 for three of the four drugs tested (colchicine, doxorubicin, and VP16). These results are similar to the [^{3}H]LTC$_4$ transport studies discussed above.

Effect of Mutations of Cys^7 and Cys^{32} on Human MRP1 Conformation—To determine how the mutations of Cys^7 and Cys^{32} affect the function of human MRP1, we determined whether the conformation of human MRP1 has been altered by the mutations using FACS analysis. Previously, FACS analysis with monoclonal antibody as a probe has been used to determine conformational changes of P-glycoprotein (34). Recently, we developed a monoclonal antibody, IU2H10, directed against the amino terminus of human MRP1 (18). The epitope of this antibody has been mapped to S^{8}ADGSDPLWD^{17}. If the conformation of human MRP1 at the amino terminus is changed by mutations of Cys^7 and Cys^{32}, the reaction of IU2H10 to human MRP1 may be different between the wild type and mutant proteins. We thus tested the reactivity of IU2H10 to cells expressing wild type and mutant human MRP1 in comparison with the monoclonal antibody QCRL-1. As shown in Fig. 6, the IU2H10 staining profile of MRP1^{C7A} and MRP1$^{C7A/C32A}$ appears to superimpose with QCRL-1 staining, whereas the IU2H10 and QCRL-1 staining traces of MRP1^{WT} have a 10-fold difference in intensity. The IU2H10 and QCRL-1 staining traces of MRP1^{C32A} are also separated but to a much lesser degree than that of MRP1^{WT}. The difference in the extent of exposure of the IU2H10 and QCRL-1 epitope between wild type and mutant MRP1 indicates that the amino terminus of MRP1^{C7A} may have a significantly different conformation from that of MRP1^{WT}.

To confirm the above observation, we took another approach using a combination of limited trypsin digestion and Western blot probed with MRP1-specific monoclonal antibodies with known epitopes. Previously, it has been shown that there are two trypsin hypersensitive cleavage sites in human MRP1. One site is located between amino acids 920 and 930, the linker domain between MSD2 and MSD3, and the other is located around amino acid residue 250 (Fig. 1). The cleavage at the site between amino acids 920 and 930 will produce two major fragments of MRP1 (14, 15, 28, 29). The 120-kDa amino-terminal half fragment including MSD1, MSD2, and nucleotide-binding domain 1 can be detected by mAb MRPr1, and the 75–80-kDa carboxyl-terminal half fragments including MSD3 and nucleotide-binding domain 2 can be detected by mAb QCRL-1. Further cleavage of the 120-kDa amino-terminal half fragments around amino acid residue 250 will generate 40–60-kDa polypeptides detected by MRPr1. As shown in Fig. 7,

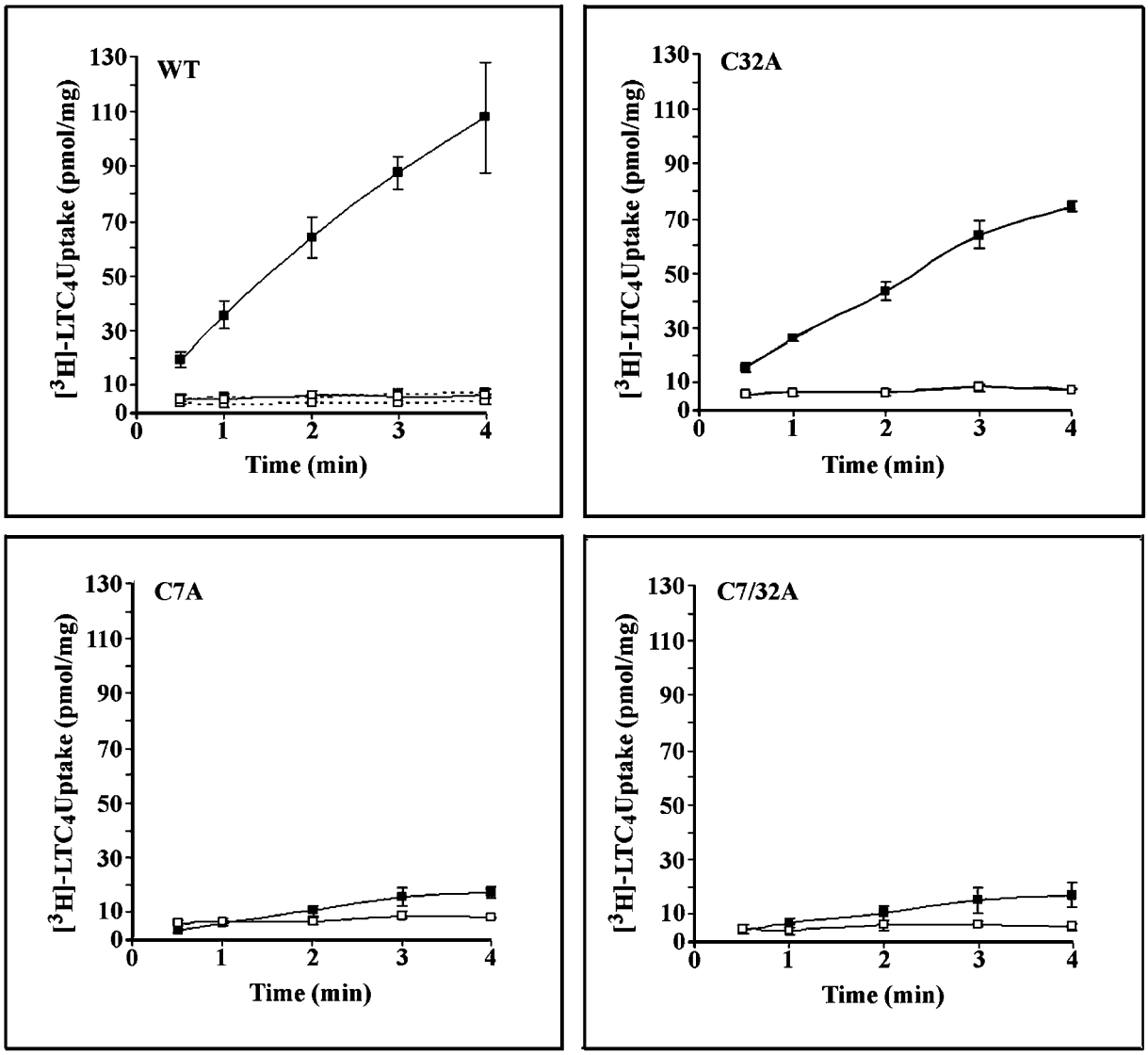

FIG. 4. **[^{3}H]LTC$_4$ uptake in membrane vesicles containing wild type and mutant human MRP1.** Membrane vesicles from cells expressing human MRP1^{WT}, MRP1^{C7A}, MRP1^{C32A}, and MRP1$^{C7A/C32A}$ were incubated with [^{3}H]LTC$_4$ in the presence of ATP (*closed symbols*) or AMP (*open symbols*) for the time indicated. The results shown are the means ± S.D. of triplicate determinations in a representative experiment and were corrected for the protein expression level as shown in Fig. 2.

TABLE I
Kinetics parameters of LTC$_4$ transport by vesicles from transfectants expressing MRP1^{WT}, MRP1^{C7A}, MRP1^{C32A}, and MRP1$^{C7A/C32A}$

	K_m	V_{max}	V_{max} (corrected)
MRP1^{WT}	194 ± 20	89 ± 9	89
MRP1^{C7A}	175 ± 20	67 ± 13	13
MRP1^{C32A}	175 ± 48	116 ± 23	83
MRP1$^{C7A/C32A}$	176 ± 12	137 ± 26	16

limited trypsin digestion of membrane vesicles containing wild type and mutant MRP1 produced the amino-terminal half fragment (~120 kDa) and its further degradation products (40–60 kDa) detected by antibody MRPr1 (Fig. 7, *top panel*) together with the carboxyl-terminal half fragment (~75–80 kDa) detected by antibody QCRL-1 (Fig. 7, *bottom panel*). These results are consistent with previous observations (14, 15, 28, 29). However, MRP1^{C7A} and MRP1$^{C7A/C32A}$ mutants generated additional peptide fragments (~23 and 97 kDa) detected by MRPr1 that were not observed with MRP1^{WT} (see the peptides indicated by *arrowheads* in the *top panel* of Fig. 7). This observation suggests that the conformation of human MRP1 at the amino terminus may be altered by the mutation of Cys^7 residue. A relatively minute quantity of the 23- and 97-kDa peptides were also produced from MRP1^{C32A}, suggesting that the conformation at the amino terminus of human MRP1^{C32A} has also been changed but to a much less degree as compared with MRP1^{C7A} and MRP1$^{C7A/C32A}$. These results are consistent with the FACS analysis shown above and suggest that the dramatic effect of Cys^7 mutations on human MRP1 function is likely due to the change in protein conformation possibly at the amino terminus of the protein.

Effect of Cys^7 and Cys^{32} Mutations on Disulfide Bond Formation—The effect of Cys^7 and Cys^{32} mutations on MRP1 conformation at amino terminus observed above may be due to the effect of the mutations on the formation of disulfide bonds involving these cysteine residues. To determine whether the Cys^7 → Ala mutation causes any changes in the disulfide bond formation, we first transiently expressed the wild type and mutant amino-terminal 281 amino acids representing MSD1 (MRP1^{281N}) in HEK293 cells, and crude membranes were prepared from these cells. The crude membranes were then treated with SDS-PAGE sample buffer with or without 100 mM

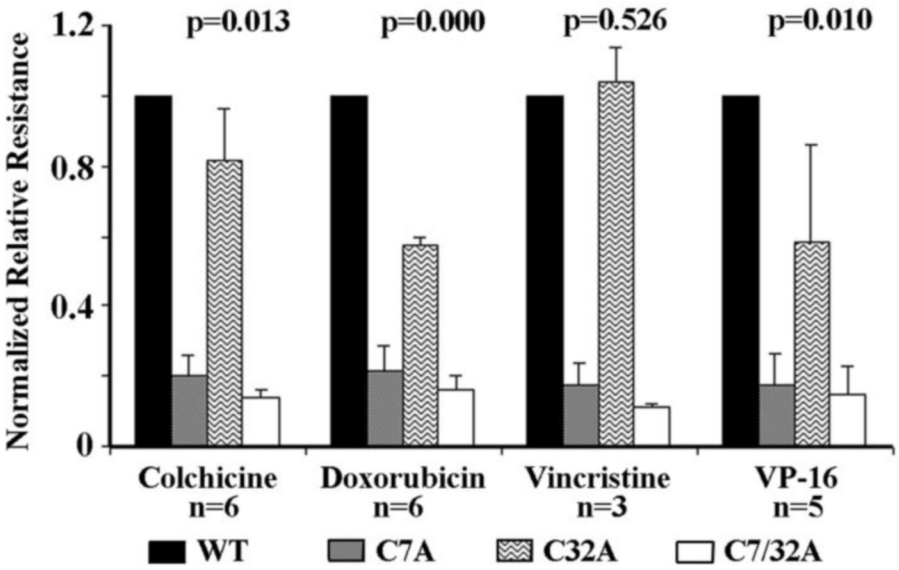

FIG. 5. **Relative drug resistance of cells expressing wild type and mutant human MRP1.** Stable HEK293 transfectants expressing human $MRP1^{WT}$, $MRP1^{C7A}$, $MRP1^{C32A}$, and $MRP1^{C7A/C32A}$ were tested for their resistance to colchicine, doxorubicin, vincristine, and VP16 at different concentrations using a 3-(4,5-dimethylthiazol-2-yl)-2,5-diphenyltetrazolium bromide assay. The relative resistance level was obtained using IC_{50} corrected for MRP expression level and was normalized to that of $MRP1^{WT}$. The *p* values are for the $MRP1^{C32A}$ mutant only.

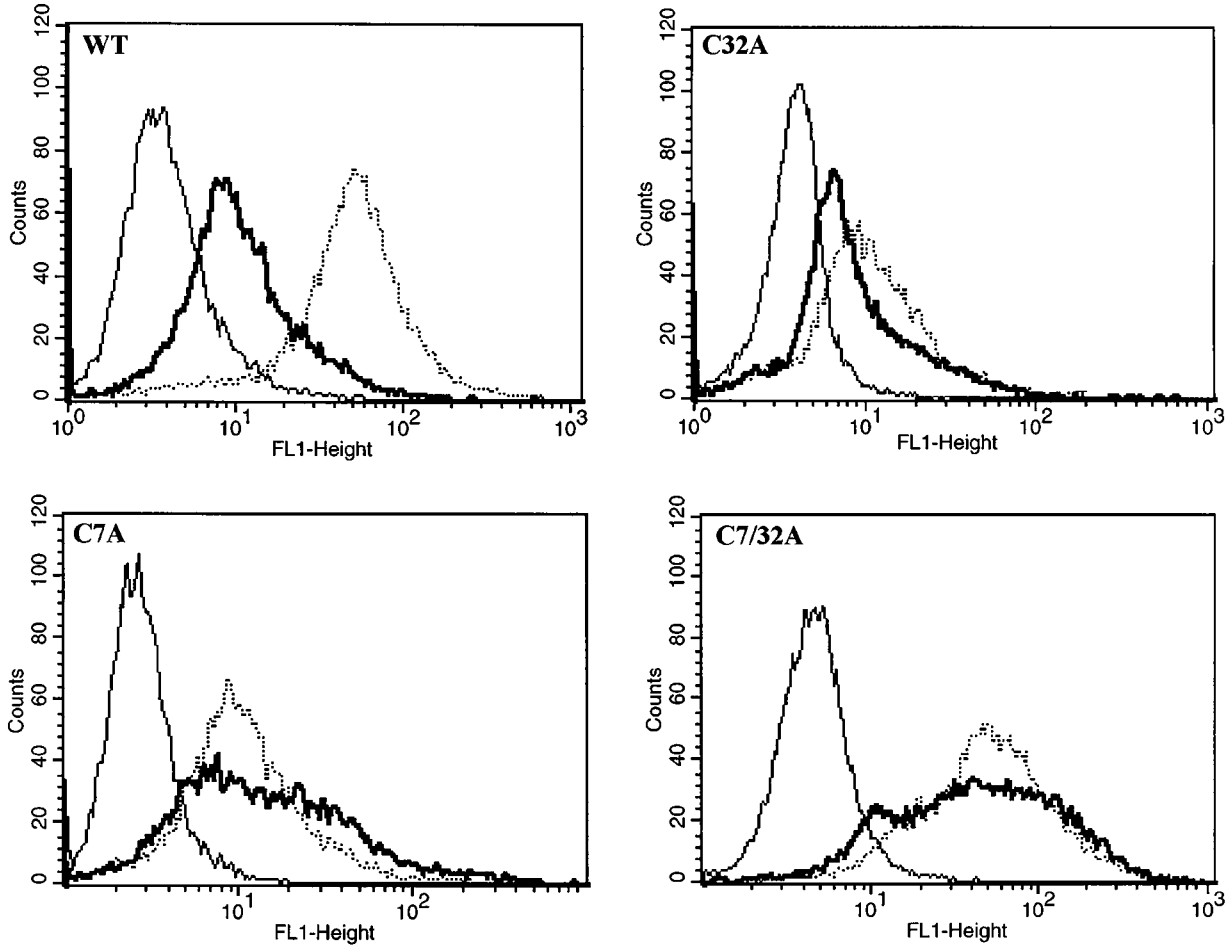

FIG. 6. **FACS analysis of wild type and mutant human MRP1-transfected HEK293 cells.** Stable HEK293 transfectants expressing human $MRP1^{WT}$, $MRP1^{C7A}$, $MRP1^{C32A}$, and $MRP1^{C7A/C32A}$ were probed with irrelevant antibody IU15H6 (*thin solid line*), MRP1-specific antibody IU2H10 (*thick solid line*), and QCRL-1 (*dotted line*) in the presence of 0.2% saponin followed by incubation with FITC-conjugated anti-mouse IgG for FACS analysis.

DTT at room temperature for 30 min and then subjected to SDS-PAGE and Western blot analysis. As shown in Fig. 8*A*, the $MRP1^{281N-WT}$ formed dimers under nonreducing conditions (Fig 8*A*, *lane 1*) that disappeared in the presence of DTT (Fig. 8*A*, *lane 2*), suggesting that intermolecular disulfide bonds may be formed between $MRP1^{281N-WT}$ molecules. However, the full-length MRP1 does not have intermolecular disulfide bonds (Fig. 9). Thus, formation of the intermolecular disulfide bond in the truncated $MRP1^{281N-WT}$ must be due to the change in the folding of the MSD1 domain in the absence of the carboxyl-terminal core domain (see below).

Interestingly, mutation of Cys^7 ($MRP1^{281N-C7A}$ and

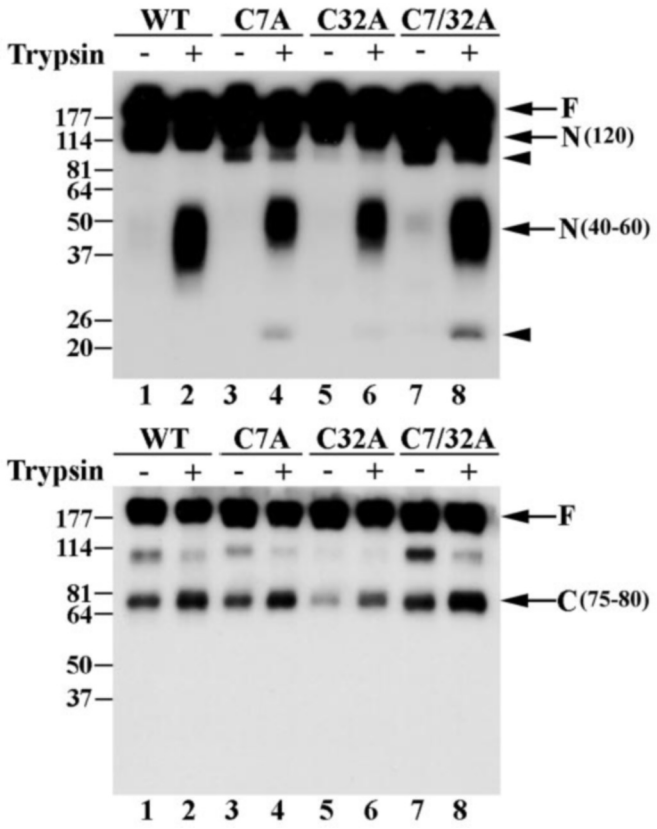

FIG. 7. **Limited trypsin digestion of wild type and mutant human MRP1.** 10 μg of membrane proteins from cells expressing human $MRP1^{WT}$, $MRP1^{C7A}$, $MRP1^{C32A}$, and $MRP1^{C7A/C32A}$ were digested with trypsin, and the membrane-associated fragments were then pelleted for SDS-PAGE and Western blot analysis using monoclonal antibody MRPr1 (*top panel*) and QCRL-1 (*bottom panel*). Undigested full-length (*F*) and the digested amino-terminal half (*N*) and carboxyl-terminal half (*C*) fragments are indicated by *arrows*. Note that the half molecules were also produced prior trypsin digestions caused by degradation in the absence of protease inhibitors in the assay. The *arrowheads* indicate the fragments produced only from the mutant human MRP1.

$MRP1^{281N\text{-}C7A/C32A}$) significantly reduced the dimer formation (Fig. 8, *A*, *lanes 3* and *7* and *B*), whereas mutation of Cys^{32} ($MRP1^{281N\text{-}C32A}$) did not (Fig. 8, *A*, *lane 5*, and *B*) under nonreducing conditions. These results indicate that Cys^7 either is responsible for the formation of the intermolecular disulfide bond of MSD1 ($MRP1^{281N}$) or plays an important role in the folding of the MSD1, and its mutation causes the change in conformation that reduces the formation of intermolecular disulfide bonds.

It has been reported previously that co-expression of the MSD1 ($MRP1^{281N}$) and the carboxyl-terminal core domain molecule of MRP1 can generate functional molecules, whereas the core domain alone is not functional (19, 20). The results in Fig. 8 suggest that MSD1 ($MRP1^{281N\text{-}WT}$) may not fold correctly when expressed alone. To test this possibility, we determined the effect of co-expressing the carboxyl-terminal core domain on the formation of the intermolecular disulfide bonds in $MRP1^{281N\text{-}WT}$ molecules. The constructs encoding the $MRP1^{281N\text{-}WT}$ and the core domain ($MRP1^{CORE}$) were co-transfected transiently into HEK293 cells. Crude membranes were prepared from the cells expressing both $MRP1^{281N\text{-}WT}$ and $MRP1^{CORE}$ and were used for nonreducing gel analysis in comparison with cells expressing only $MRP1^{281N\text{-}WT}$ or $MRP1^{CORE}$. As shown in Fig. 9, expression of $MRP1^{281N\text{-}WT}$ was detected by monoclonal antibody MRPr1 in the cells transfected with $MRP1^{281N\text{-}WT}$ or both $MRP1^{281N\text{-}WT}$ and $MRP1^{CORE}$ but not in cells transfected with $MRP1^{CORE}$ alone (Fig. 9*A*, compare *lanes 3–8*). On the other hand, expression of $MRP1^{CORE}$ was detected by monoclonal antibody QCRL-1 in the cells transfected with $MRP1^{CORE}$ or both $MRP1^{281N\text{-}WT}$ and $MRP1^{CORE}$ but not in cells transfected with $MRP1^{281N\text{-}WT}$ alone (Fig. 9*B*, compare *lanes 3–8*). Interestingly, the dimer formed by $MRP1^{281N\text{-}WT}$ under nonreducing conditions (Fig. 9*A*, *lane 3*) disappeared in the presence of $MRP1^{CORE}$ (Fig. 9*A*, *lane 5*). Thus, the folding of the $MRP1^{281N\text{-}WT}$ is different in the presence and absence of the core domain. Furthermore, no apparent full-length molecules consisting of $MRP1^{281N\text{-}WT}$ and $MRP1^{CORE}$ were detected under nonreducing conditions (Fig. 9, *A* and *B*, *lanes 5* and *6*). Thus, no disulfide bonds may be formed between the amino-terminal MSD1 ($MRP1^{281N\text{-}WT}$) and the carboxyl-terminal core domain ($MRP1^{CORE}$). It is also noteworthy that no apparent dimers between the full-length human MRP1 are observed under nonreducing conditions (Fig. 9, *A* and *B*, *lanes 1* and *2*), suggesting that there are no intermolecular disulfide bonds in the full-length human MRP1.

DISCUSSION

In this study, we found that the two cysteine residues in the putative extracellular amino terminus (Cys^7 and Cys^{32} in human MRP1) are conserved among the five human MRPs (MRP1, 2, 3, 6, and 7) that have the additional membrane spanning domain (MSD1) compared with the other human MRPs, which do not have MSD1. We examined whether these two cysteine residues are structurally and functionally important by site-directed mutagenesis and found that mutation of the Cys^7 residue reduced more than 80% of MRP1-mediated LTC_4 transport and drug resistance to colchicine, doxorubicin, vincristine, and VP16. On the other hand, mutation of the Cys^{32} residue reduced only about 20% of MRP1-mediated LTC_4 transport and 20–40% of resistance to colchicine, doxorubicin, and VP16. It had no effect on resistance to vincristine. We also found that Cys^7 is essential for maintaining the structural integrity of human MRP1 and that its mutation affects the folding and conformation of the MSD1 domain.

The observation that the mutation of the Cys^7 residue reduced significantly the V_{max} of [^{3}H]LTC_4 transport but did not affect the K_m suggests that the Cys^7 mutation likely influences the substrate turnover rate but not the [^{3}H]LTC_4 binding affinity to MRP1. The loss of resistance activity of $MRP1^{C7A}$ to colchicine, doxorubicin, vincristine, and VP16 may also be due to the effect on the substrate turnover rate. This effect on function by Cys^7 mutation is likely due to the influence of the mutation on the structural integrity at the amino terminus of human MRP1 as discussed below. Possibly, the $Cys^7 \rightarrow$ Ala mutation results in a conformation at the amino terminus that crippled the substrate turnover rate of the protein, although the protein may still bind the drug substrates.

It has been shown previously that MRP1 has at least two drug-binding sites (35) and that these putative drug-binding sites are likely located in the transmembrane segments 10 and 11 in MSD2 and segments 16 and 17 in MSD3 (29, 36), similar to that found in P-glycoprotein (37–39). The MSD1 domain including the putative amino terminus is not labeled by photo affinity substrates, and its absence does not affect LTC_4 labeling of MRP1 (36). Thus, it was thought that MSD1 including the amino terminus does not involve drug binding. These observations are consistent with our conclusion that $Cys^7 \rightarrow$ Ala mutation may not affect drug binding. However, in this study we also found that $Cys^{32} \rightarrow$ Ala mutation did not affect MRP1-mediated resistance to vincristine, whereas the resistance activity of $MRP1^{C32A}$ to colchicine, doxorubicin, and VP16 was reduced about 20–40%, suggesting that Cys^{32} in the amino terminus of human MRP1 may participate in substrate recog-

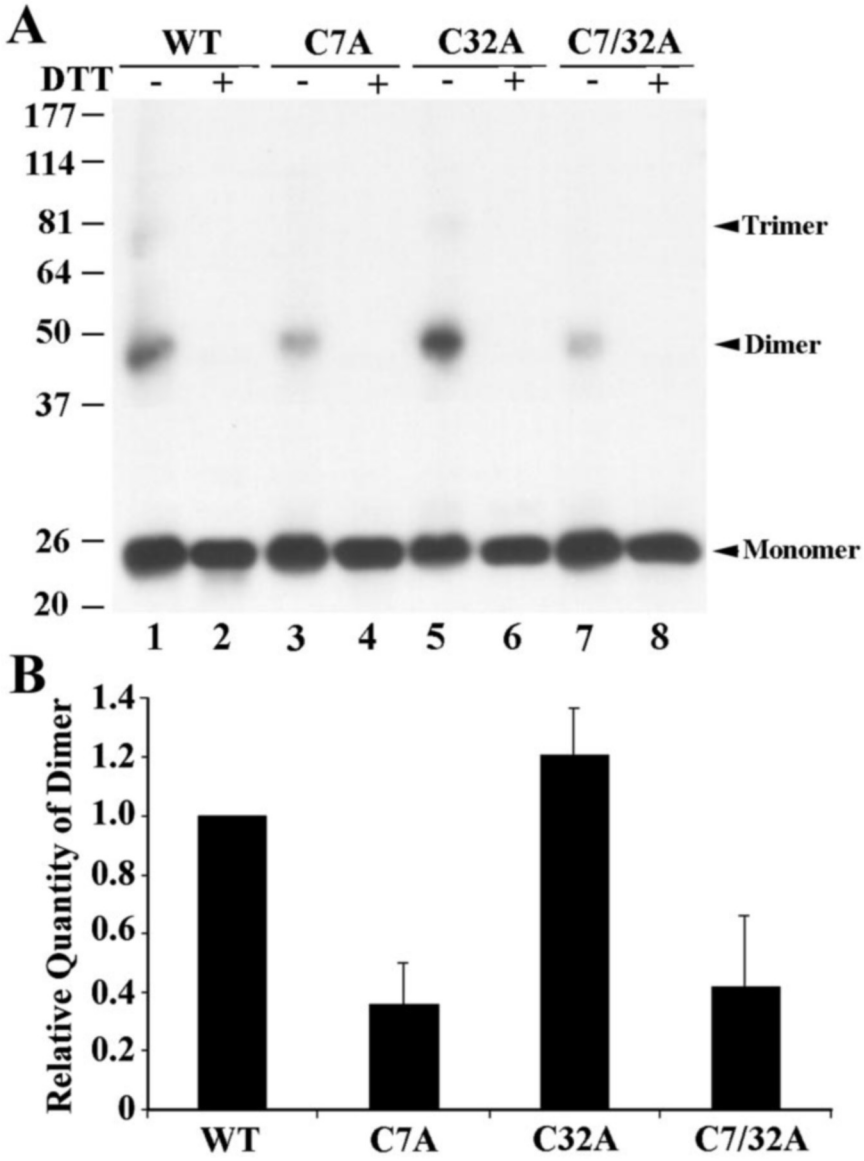

FIG. 8. **Effect of cysteine mutations on disulfide bond formation.** Crude membranes from transiently transfected HEK293 cells expressing human $MRP1^{281N\text{-}WT}$, $MRP1^{281N\text{-}C7A}$, $MRP1^{281N\text{-}C32A}$, and $MRP1^{281N\text{-}C7A/C32A}$ were treated with SDS-PAGE sample buffer in the absence or presence of 100 mM DTT before being subjected to SDS-PAGE and Western blot analysis using monoclonal antibody MRPr1 as a probe (*A*). *B* shows the relative quantity of dimers generated from four independent experiments. The intensity of the dimer product (*DTT* −) and the total protein (*DTT* +) was determined using Scion image software. The relative quantities of the dimer are presented as fractions generated by dividing the intensity of the dimers with the intensity of the total protein and normalized to that of the $MRP1^{281N\text{-}WT}$.

nition. Clearly, further experiments are needed to clarify these differences and to determine whether MSD1 including the amino terminus is involved in substrate recognition and binding.

In a previous study, Gao *et al.* (19) found that deletion of as few as 66 amino acids of the amino terminus of human MRP1 reduced 90% of LTC_4 transport activity of MRP1. This observation is consistent with the results of the Cys^7 mutation in this study. However, it has also been concluded from previous domain deletion studies that MSD1 with the amino terminus is not necessary for the LTC_4 transport activity of MRP1 (20). Therefore, it remains to be answered why MRP1 has the MSD1 if this domain does not contribute to the function of MRP1. It is possible that the amino terminus of the MSD1 contains positive elements for MRP1 function and deletion or mutation of these elements will significantly reduce MRP1 activity. On the other hand, deletion of the entire MSD1 may delete other negative elements in the MSD1 together with the positive element at the amino terminus for LTC_4 transport activity. Interestingly, it was also found that the loop (L_0) linking MSD1 and MSD2 appears to be essential for LTC_4 transport activity. Therefore, further manipulations of MSD1 with mutagenesis may help dissect the functional role and the crucial elements in the MSD1 for MRP1 activity.

Limited trypsin digestion of both wild type and mutant human MRP1 generated a 120-kDa amino-terminal half fragment detected by a monoclonal antibody MRPr1 and a ~75–80-kDa carboxyl-terminal half fragment detected by monoclonal antibody QCRL-1. Fragments of 40–60 kDa were also produced from both wild type and mutant human MRP1. These observations are consistent with previous studies (14, 15, 28, 29). However, digestion of $MRP1^{C7A}$ mutant also generated additional fragments of 23 and 97 kDa detected by MRPr1. A relatively minute quantity of these two fragments was also produced from digestion of $MRP1^{C32A}$ but not from $MRP1^{WT}$. Generation of these two fragments is possibly due to digestion at Arg^{62} and/or Lys^{72} (Fig. 1*A*, trypsin site 3) in the first cytoplasmic loop. Likely, the 23- and 97-kDa fragments span from trypsin site 3 to trypsin site 2 (near amino acid residue 250) and from trypsin site 3 to trypsin site 1 (between amino acids 920 and 930), which carry the MRPr1 epitope (Fig. 1*A* for trypsin sites). Generation of these additional fragments by digestion of mutant MRP1 suggests that the conformation of human MRP1 at the amino terminus has been altered by the $Cys^7 \rightarrow Ala$ mutation and to a significantly less degree by the $Cys^{32} \rightarrow Ala$ mutation. These results are consistent with the

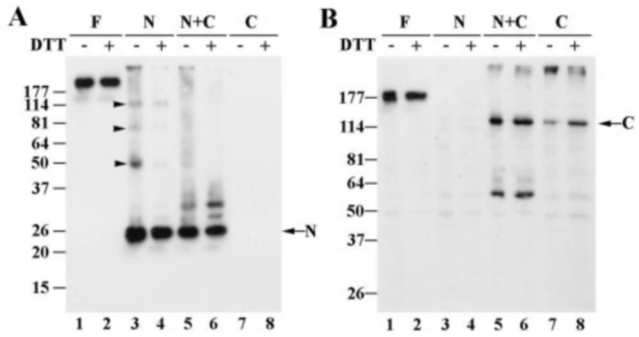

FIG. 9. **Co-expression of human MRP1$^{281N\text{-}WT}$ and MRP1^{CORE}.** 2.5-μg membranes from HEK293 cells transiently transfected with MRP1$^{281N\text{-}WT}$, MRP1^{CORE}, or both were treated with SDS-PAGE sample buffer in the presence or absence of 100 mM DTT and then subjected to SDS-PAGE and Western blot analysis with monoclonal antibody MRPr1 (*A*) and QCRL-1 (*B*). *F*, full-length human MRP1^{WT}; *N*, human MRP1$^{281N\text{-}WT}$; *C*, human MRP1^{CORE}. The *arrows* indicate MRP1$^{281N\text{-}WT}$ (*A*) and MRP1^{CORE} (*B*) products. The oligomers of MRP1^{281N} formed in the absence of DTT are shown by *arrowheads*.

cell staining data using monoclonal antibody, IU2H10, which generated different profiles of staining for wild type and mutant human MRP1.

We also found that the correct folding of MSD1 (MRP1^{281N}) requires the presence of the carboxyl-terminal core domain (MRP1^{CORE}). Without the core domain, MSD1 forms intermolecular disulfide bond. In the presence of the core domain, no such disulfide bond is formed. These observations suggest that the folding of MSD1 is different in the absence and presence of the core domain. It has been shown previously that functional MRP1 was produced when the MSD1 and the core domain were co-expressed (19). We thus conclude that the folding of the MSD1 in the presence of the core domain is likely correct and that the folding of MSD1 in the absence of the core domain is incorrect, which results in the formation of intermolecular disulfide bonds. Mutation of the Cys^7 residue inhibited the formation of these intermolecular disulfide bonds of MSD1 in the absence of the core domain. Thus, it is possible that the conformation of the MSD1 is changed by the Cys^7 mutation in such a way that the intermolecular disulfide bond cannot be formed any more. This notion supports the conclusion that the Cys^7 mutation changes the conformation of the amino terminus as discussed above.

However, it is also possible that the Cys^7 residue directly contributes to the formation of the intermolecular disulfide bonds of MSD1 in the absence of the core domain and that its mutation eliminated the intermolecular disulfide bond formation. If this were the case, it would be possible that the Cys^7 residue may be an active Cys and that it may normally form a disulfide bond with another Cys residue in the full-length MRP1. Upon deletion of the core domain, the Cys partner for Cys^7 would be deleted. However, we found no apparent formation of intermolecular disulfide bond between MSD1 (MRP1$^{281N\text{-}WT}$) and the carboxyl-terminal core domain (MRP1^{CORE}) when the two domains were co-expressed. Thus, in the full-length MRP1 molecule, Cys^7 may stay with a free SH group, or it may form a disulfide bond with a Cys residue in the MSD1 or in other proteins. Formation of a disulfide bond between Cys^7 and other proteins is unlikely because the mobility of full-length human MRP1 on SDS-PAGE was not decreased in the absence of DTT (Fig. 9). Furthermore, although the Cys^7 → Ala mutation reduced 80% of MRP1-mediated LTC_4 transport and drug resistance activity, Cys^{32} → Ala mutation reduced only 20% of MRP1-mediated LTC_4 transport and resistance to some drug substrates. Thus, it appears that the effect of mutations on MRP1 function is not simply due to the disruption of the potential Cys^7–Cys^{32} disulfide bond. However, the MSD1 domain has seven additional Cys residues, and one of these residues may be a potential partner of Cys^7. Thus, it is possible that MSD1 misfolds in the absence of the core domain. Because of this misfolding, Cys^7 cannot form disulfide bond with its normal partner, which resulted in misoxidation possibly with itself in another MSD1 molecule.

The extracellular location of the amino terminus of human MRP1 has been inferred by determining the glycosylation status and epitope insertion (14–17). However, using a monoclonal antibody, IU2H10, which has the epitope ^{8}SADGSDPLWD[17] in the amino terminus of human MRP1, we found that at least part of the amino terminus (IU2H10 epitope) of human MRP1 may be exposed cytoplasmically (18) (Fig. 1*B*). In this new model, Cys^7 may be located in a channel formed by the transmembrane segments of the protein. We also found that the cytoplasmic retraction of the amino terminus of human MRP1 depends on the presence of the carboxyl-terminal core domain (18). As discussed above, the finding that the intermolecular disulfide bond formation between MSD1 is inhibited by the presence of the carboxyl-terminal core domain suggests that the correct folding of the amino terminus requires the presence of the carboxyl-terminal core domain. This observation is consistent with the observation that the cytoplasmic retraction of Cys^7 also requires the presence of the carboxyl-terminal core domain (18).

Previously, Cys-less mutant P-glycoprotein (Cys → Ala mutations) has been used successfully for identification of residues in drug-binding domain (40, 41), determination of the drug-binding domain dimension (42), functional analysis of nucleotide-binding domain (43), and topology mapping (44). These successful studies demonstrate that cysteine-scanning mutagenesis is a powerful tool to examine the structure and function of membrane transport proteins. However, these studies depended on the fact that mutation of all Cys residues to Ala did not affect the function of human P-glycoprotein (44). Based on the present study, it is conceivable that such a cysteine-scanning mutagenesis approach is unlikely to work for the full-length human MRP1 unless mutations of other Cys residues restore the effects of the Cys^7 and Cys^{32} mutations.

Site-directed mutagenesis has been used to examine the functional domains of human MRP1. Glu^{1089} in the transmembrane segment 14 of human MRP1 was found to be an essential residue for anthracycline resistance (25). Mutation of Glu^{1089} to neutral amino acids reduced the anthracycline resistance of MRP1, whereas mutation to positively charged amino acids completely eliminated anthracycline resistance. Yet, these mutations had no effect on transport of conjugated organic anions such as LTC_4. Thr^{1242} in the transmembrane segment 17 of human MRP1 was also found to be important for MRP1 function (26). Mutation of Thr^{1242} reduced MRP1-mediated transport of LTC_4 and $E_2$17βG and drug resistance. Interestingly, double mutations of Glu^{1089} and Thr^{1242} restored the effect of Thr^{1242} mutation alone, suggesting that there may be an interaction between transmembrane segments 14 and 17. Mutations of Trp^{1246} in the transmembrane segment 17, which is conserved between human and mouse MRP1, also generated proteins that do not confer resistance to anticancer drugs as the wild type protein, notwithstanding that they still transport LTC_4 (32). Although these studies collectively demonstrated that some amino acid residues in the transmembrane segments are important for drug specificity and transport function of human MRP1, it is not known whether these mutations affect the folding and conformation of MRP1. However, we demonstrated in this study that mutations of Cys^7 reduced MRP1-mediated LTC_4 transport and resistance to anticancer drugs

likely because of the change in conformation of MRP1. Based on these previous studies, it will be interesting in the future to determine whether mutation of other Cys residues in MSD1 can compensate the effect of the Cys^{7} mutation.

Currently, we cannot rule out the possibility that the effect of mutation of Cys residues to Ala on the conformation and function of MRP1 in this study is due to the presence of Ala residues. Additional substitutions of Cys with other residues such as Ser and Met may help address this issue. However, analysis of the amino-terminal sequence of human MRP1 using several programs (www.expasy.ch/tools/#secondary) predicts that it mainly consists of coiled structures with a short stretch of β strand (Fig. 1*B*). Both Cys^{7} and Cys^{32} are located in the domain consisting of coiled structures. Replacing both Cys residues with Ala does not change the overall coil structure of the amino terminus as predicted using the same program discussed above. Thus, it is unlikely that the effect of a Cys → Ala mutation on the structure and function of human MRP1 was simply due to the presence of Ala residues.

Acknowledgments—We thank other members of our laboratory for valuable discussion over the course of this study. We also thank Dr. Piet Borst for the human MRP1 cDNA. Critical reading of the manuscript and suggestions from Dr. Guillermo Altenberg are greatly appreciated.

REFERENCES

1. Cole, S. P., Bhardwaj, G., Gerlach, J. H., Mackie, J. E., Grant, C. E., Almquist, K. C., Stewart, A. J., Kurz, E. U., Duncan, A. M., and Deeley, R. G. (1992) *Science* **258,** 1650–1654
2. Higgins, C. F. (1992) *Annu. Rev. Cell Biol.* **8,** 67–113
3. Theodoulou, F. L. (2000) *Biochim. Biophys. Acta* **1465,** 79–103
4. Dean, M., Rzhetsky, A., and Allikmets, R. (2001) *Genome Res.* **11,** 1156–1166
5. Litman, T., Druley, T. E., Stein, W. D., and Bates, S. E. (2001) *Cell. Mol. Life Sci.* **58,** 931–959
6. Buchler, M., Konig, J., Brom, M., Kartenbeck, J., Spring, H., Horie, T., and Keppler, D. (1996) *J. Biol. Chem.* **271,** 15091–15098
7. Belinsky, M., Bain, L., Balsara, B., Testa, J., and Kruh, G. (1998) *J. Natl. Cancer Inst.* **90,** 1735–1741
8. Longhurst, T. J., O'Neill, G. M., Harvie, R. M., and Davey, R. A. (1996) *Br. J. Cancer* **74,** 1331–1335
9. Lee, K., Belinsky, M. G., Bell, D. W., Testa, J. R., and Kruh, G. D. (1998) *Cancer Res.* **58,** 2741–2747
10. Hopper, E., Belinsky, M. G., Zeng, H., Tosolini, A., Testa, J. R., and Kruh, G. D. (2001) *Cancer Lett.* **162,** 181–191
11. Bera, T. K., Lee, S., Salvatore, G., Lee, B., and Pastan, I. H. (2001) *Mol. Med.* **7,** 509–516
12. Hipfner, D. R., Deeley, R. G., and Cole, S. P. C. (1999) *Biochim. Biophys. Acta* **1461,** 359–376
13. Tusnady, G. E., Bakos, E., Varadi, A., and Sarkadi, B. (1997) *FEBS Lett.* **402,** 1–3
14. Bakos, E., Hegedus, T., Hollo, Z., Welker, E., Tusnady, G. E., Zaman, G. J., Flens, M. J., Varadi, A., and Sarkadi, B. (1996) *J. Biol. Chem.* **271,** 12322–12326
15. Hipfner, D. R., Almquist, K. C., Leslie, E. M., Gerlach, J. H., Grant, C. E., Deeley, R. G., and Cole, S. P. (1997) *J. Biol. Chem.* **272,** 23623–23630
16. Kast, C., and Gros, P. (1997) *J. Biol. Chem.* **272,** 26479–26487
17. Zhang, J. T. (2000) *Biochem. J.* **348,** 597–606
18. Chen, Q., Yang, Y., Liu, Y., Han, B., and Zhang, J. T. (2002) *Biochemistry* **41,** 9052–9062
19. Gao, M., Yamazaki, M., Loe, D. W., Westlake, C. J., Grant, C. E., Cole, S. P. C., and Deeley, R. G. (1998) *J. Biol. Chem.* **273,** 10733–10740
20. Bakos, E., Evers, R., Szakacs, G., Tusnady, G. E., Welker, E., Szabo, K., de Haas, M., van Deemter, L., Borst, P., Varadi, A., and Sarkadi, B. (1998) *J. Biol. Chem.* **273,** 32167–32175
21. Bakos, E., Evers, R., Calenda, G., Tusnady, G. E., Szakacs, G., Varadi, A., and Sarkadi, B. (2000) *J. Cell Sci.* **113,** 4451–4461
22. Zhang, M., Wang, G., Shapiro, A., and Zhang, J. T. (1996) *Biochemistry* **35,** 9728–9736
23. Loe, D. W., Almquist, K. C., Deeley, R. G., and Cole, S. P. (1996) *J. Biol. Chem.* **271,** 9675–9682
24. Stride, B. D., Cole, S. P., and Deeley, R. G. (1999) *J. Biol. Chem.* **274,** 22877–22883
25. Zhang, D.-W., Cole, S. P. C., and Deeley, R. G. (2001) *J. Biol. Chem.* **276,** 13231–13239
26. Zhang, D.-W., Cole, S. P. C., and Deeley, R. G. (2001) *J. Biol. Chem.* **276,** 34966–34974
27. Wang, G., Pincheira, R., Zhang, M., and Zhang, J. T. (1997) *Biochem. J.* **328,** 897–904
28. Hipfner, D. R., Almquist, K. C., Stride, B. D., Deeley, R. G., and Cole, S. P. (1996) *Cancer Res.* **56,** 3307–3314
29. Daoud, R., Julien, M., Gros, P., and Georges, E. (2001) *J. Biol. Chem.* **276,** 12324–12330
30. Stride, B. D., Grant, C. E., Loe, D. W., Hipfner, D. R., Cole, S. P., and Deeley, R. G. (1997) *Mol. Pharmacol.* **52,** 344–353
31. Prechtl, S., Roellinghoff, M., Scheper, R., Cole, S. P., Deeley, R. G., and Lohoff, M. (2000) *J. Immunol.* **164,** 754–761
32. Ito, K.-I., Olsen, S. L., Qiu, W., Deeley, R. G., and Cole, S. P. C. (2001) *J. Biol. Chem.* **276,** 15616–15624
33. Manciu, L., Chang, X., Riordan, J. R., Buyse, F., and Ruysschaert, J. M. (2001) *FEBS Lett.* **493,** 31–35
34. Mechetner, E. B., Schott, B., Morse, B. S., Stein, W. D., Druley, T., Davis, K. A., Tsuruo, T., and Roninson, I. B. (1997) *Proc. Natl. Acad. Sci. U. S. A.* **94,** 12908–12913
35. Daoud, R., Desneves, J., Deady, L. W., Tilley, L., Scheper, R. J., Gros, P., and Georges, E. (2000) *Biochemistry* **39,** 6094–6102
36. Qian, Y.-M., Qiu, W., Gao, M., Westlake, C. J., Cole, S. P. C., and Deeley, R. G. (2001) *J. Biol. Chem.* **276,** 38636–38644
37. Bruggemann, E. P., Germann, U. A., Gottesman, M. M., and Pastan, I. (1989) *J. Biol. Chem.* **264,** 15483–15488
38. Greenberger, L. M., Lisanti, C. J., Silva, J. T., and Horwitz, S. B. (1991) *J. Biol. Chem.* **266,** 20744–20751
39. Zhang, X., Collins, K. I., and Greenberger, L. M. (1995) *J. Biol. Chem.* **270,** 5441–5448
40. Loo, T. W., and Clarke, D. M. (1999) *J. Biol. Chem.* **274,** 35388–35392
41. Loo, T. W., and Clarke, D. M. (2000) *J. Biol. Chem.* **275,** 39272–39278
42. Loo, T. W., and Clarke, D. M. (2001) *J. Biol. Chem.* **276,** 36877–36880
43. Loo, T. W., and Clarke, D. M. (2000) *J. Biol. Chem.* **275,** 19435–19438
44. Loo, T. W., and Clarke, D. M. (1995) *J. Biol. Chem.* **270,** 843–848